

2



Lawrence Berkeley Laboratory

UNIVERSITY OF CALIFORNIA

Materials & Chemical Sciences Division

RECEIVED
LAWRENCE
BERKELEY LABORATORY

APR 19 1988

LIBRARY AND
DOCUMENTS SECTION

Submitted to Physical Review B

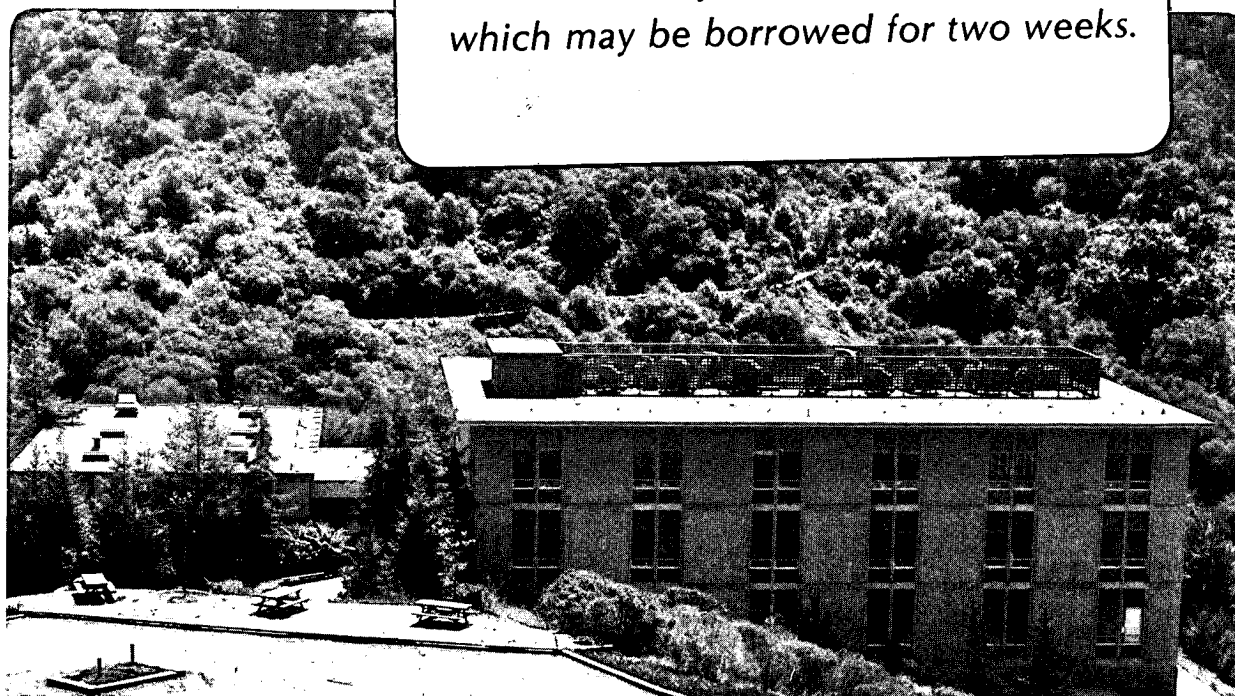
Heavy-Fermion System: Superconducting and Magnetic Fluctuations within a Periodic-Cluster Hubbard Model

A. Reich and L.M. Falicov

February 1988

TWO-WEEK LOAN COPY

*This is a Library Circulating Copy
which may be borrowed for two weeks.*



LBL-24794
2

DISCLAIMER

This document was prepared as an account of work sponsored by the United States Government. While this document is believed to contain correct information, neither the United States Government nor any agency thereof, nor the Regents of the University of California, nor any of their employees, makes any warranty, express or implied, or assumes any legal responsibility for the accuracy, completeness, or usefulness of any information, apparatus, product, or process disclosed, or represents that its use would not infringe privately owned rights. Reference herein to any specific commercial product, process, or service by its trade name, trademark, manufacturer, or otherwise, does not necessarily constitute or imply its endorsement, recommendation, or favoring by the United States Government or any agency thereof, or the Regents of the University of California. The views and opinions of authors expressed herein do not necessarily state or reflect those of the United States Government or any agency thereof or the Regents of the University of California.

HEAVY-FERMION SYSTEM: SUPERCONDUCTING AND MAGNETIC
FLUCTUATIONS WITHIN A PERIODIC-CLUSTER HUBBARD MODEL*

Ariel Reich and L. M. Falicov

Department of Physics and Materials and Chemical Sciences Division,
Lawrence Berkeley Laboratory, University of California,
Berkeley, CA 94720

and

Nordisk Institut for Teoretisk Atomfysik (NORDITA)
Blegdamsvej 17
DK-2100 Copenhagen Ø, Denmark

February 1988

*This work was supported in part by the Director, Office of Energy Research, Office of Basic Energy Sciences, Materials Sciences Division, of the U.S. Department of Energy under Contract No. DE-AC03-76SF00098.

Heavy-Fermion System: Superconducting and Magnetic Fluctuations within a Periodic-Cluster Hubbard Model

Ariel Reich and L.M. Falicov

Physics Department, and
Materials and Chemical Sciences Division, Lawrence Berkeley Laboratory,
University of California,
Berkeley, CA 94720,

and

Nordisk Institut for Teoretisk Atomfysik (NORDITA),
Blegdamsvej 17,
DK-2100 Copenhagen Ø , Denmark

(Submitted Feb. 5, 1987)

ABSTRACT

An exact solution of an eight-site crystal model with periodic boundary conditions, a small face-centered cubic crystal, is presented for the case of a heavy-fermion system. The model consists of: (a) a single, fully symmetric orbital per site, with nearest-neighbor and second nearest-neighbor hopping; (b) an *infinite* Coulomb repulsion between electrons on the same site; (c) antiferromagnetic superexchange interactions; and (d) band fillings near half-filling (six, seven and eight electrons per cluster). The superconducting and the antiferromagnetic correlations are studied and compared with the predictions of the non-interacting limit. The suitability of BCS and Gutzwiller approximate ground-state wave functions are quantitatively estimated.

February 5, 1988

PACS numbers 1988 74.70.Tx, 75.30.Mb

Heavy-Fermion System: Superconducting and Magnetic Fluctuations within a Periodic-Cluster Hubbard Model

Ariel Reich and L.M. Falicov

Physics Department, and
Materials and Chemical Sciences Division,
Lawrence Berkeley Laboratory,
University of California,
Berkeley, CA 94720,

and

Nordisk Institut for Teoretisk Atomfysik (NORDITA),
Blegdamsvej 17,
DK-2100 Copenhagen Ø , Denmark

(Submitted Feb. 5, 1987)

I. INTRODUCTION

Heavy-fermion materials, with their high heat capacities at low temperatures, exhibit sometimes normal and sometimes re-entrant superconductivity. They have been a source of great experimental and theoretical attention¹⁻⁴. This interest has been further fueled by early experimental evidence showing a degree of similarity between these and the new high-temperature superconducting ceramics, with many of the leading ideas for high T_c mechanisms borrowed from heavy-fermion research⁵⁻⁹.

One direction in the incorporation of the large Coulomb repulsion between the f -electrons of

these lanthanide and actinide heavy-fermion materials has been the use of the single-orbital-per-site Hubbard model¹⁰, or the twin-orbital-per-site Anderson model¹¹, in order to make the non-negligible many-body effects more mathematically tractable.

The current work focuses on the Hubbard model, wherein the computational overhead is further reduced by a small-cluster approach which incorporates periodic boundary conditions. This method¹² has been applied to various problems: photoemission^{13,14}, intermediate-valence^{14,15}, magnetic¹⁶, thermodynamic¹⁷, resonating-valence-bond¹⁸ and alloying behavior¹⁹. These papers have shown the approach to be good for explaining uniform and short-range correlation properties and, although incapable of exhibiting phase transitions, it has shown indications of possible mechanisms involved in them. In previous work²⁰ the present authors have explored the Fermi surface, spin-wave and transport properties of the an eight-site, seven electron fcc cluster, which proved to be similar to real heavy-fermion systems. In this contribution the small-cluster model, with various occupations, is analyzed for the superconducting-fluctuation behavior, to investigate possible mechanisms for superconductivity.

The lattice in the model is face-centered-cubic, a three-dimensional array of triangular rings, which is the classical example of an antiferromagnetically spin-frustrated system. This idea of electrons having to alternate between forming spin-singlet states with all adjacent electrons is the basis for Anderson's concept²¹ of Resonating-Valence-Bond (RVB). Thus, one way to address the relevance of the RVB approach, in the context of high- T_c superconductivity, is to examine an extreme case, such as the present one.

Section II reviews the Hamiltonian employed. Section III examines the nature of the ground and low-lying excited states, as well as the suitability of the Gutzwiller projection approach. Section IV examines the superconducting correlations, in terms of its anisotropy, degree of spontaneous-symmetry breaking, and relative strengths of various spin-coupling modes. The relation between the BCS predicted ground-state wavefunctions and the actual ones are also examined, and finally, the magnetic correlation behavior is studied.

II. THE HAMILTONIAN

The Hamiltonian is thoroughly discussed in Reference 20. The limit of large on-site Coulomb repulsion, $U \rightarrow \infty$, reduces it²²⁻²⁴ to the form:

$$H = H_{1nn} + H_{2nn} + H_{AF}, \quad (2.1)$$

where

$$H_{1nn} = -2t \sum_{\substack{i,j=0\dots7;\sigma \\ (i,j)=1nn}} c_{i\sigma}^\dagger c_{j\sigma} \quad (2.2)$$

represents first-nearest neighbor hopping, with transfer integral t ,

$$H_{2nn} = -6T \sum_{\substack{i,j=0\dots7;\sigma \\ (i,j)=2nn}} c_{i\sigma}^\dagger c_{j\sigma} \quad (2.3)$$

represents second-nearest neighbor hopping, with transfer integral T , and

$$H_{AF} = J \sum_{\substack{i,j=0\dots7 \\ (i,j)=1nn}} \vec{S}_i \cdot \vec{S}_j \quad (2.4)$$

is a Heisenberg interaction where J represents the effective antiferromagnetic coupling of order (t^2/U) .

The eight-atom cluster in the fcc structure has the symmetry of a space group with 192 operations and 13 representations. These representations are: five at the Γ point of the Brillouin zone (referred to as Γ_1 , Γ_2 , Γ_{12} , Γ_{15}' and Γ_{25}' , with degeneracies 1, 1, 2, 3, and 3, respectively), five at X (X_1 , X_2 , X_3 , X_4 , X_5 ; degeneracies 3, 3, 3, 3, and 6, respectively) and three at L (L_1 , L_2 , L_3 ; degeneracies 4, 4, and 8, respectively); the labels Γ , X and L refer to the overall \vec{k} -vector of the many-body wavefunction. The notation is the standard one of Bouckaert *et al*²⁵.

This model has been solved exactly for occupations of 6, 7 and 8 electrons (corresponding to 0.75, 0.875 and 1.0 electrons per site), and the relevant ground and low-lying states are presented in Table I. In addition the non-interacting ground and low-lying states are presented, separated according to their first-order correction in Coulomb energy, which is obtained by diagonalizing, in the $U = 0$ ground-state manifold, the operator :

$$H_C = U \sum_{i=0\dots7} c_{i\uparrow}^\dagger c_{i\uparrow} c_{i\downarrow}^\dagger c_{i\downarrow}. \quad (2.5)$$

III. THE GUTZWILLER-PROJECTED STATE

It is interesting at this point to examine the so-called Gutzwiller method^{9,26-29}. The approach approximates the interacting ground state by projecting out of the non-interacting ground-state wave function any part that contains doubly occupied sites:

$$|\Psi_G\rangle = \prod_i (1 - c_{i\uparrow}^\dagger c_{i\uparrow} c_{i\downarrow}^\dagger c_{i\downarrow}) |\Psi_0\rangle, \quad (2.6)$$

where the product index i runs over all sites. The appeal of the approach is obvious from its aesthetics to its relative ease of implementation. However, as shown before²⁰ and here, the pitfalls of such an approach become evident.

One sees the situation schematically in Figs. 1-3, depicting the ground- and low-lying excited states for occupations of 6, 7 and 8 electrons, respectively. For 6 electrons, if one follows the $^1\Gamma_{12}$ non-interacting ground state of minimal Coulomb energy, and performs the Gutzwiller projection (2.6), one arrives, at infinite U , at the proper ground state. For 7 electrons, however, the small- U ground state, if projected, yields an excited state of the heavy-fermion manifold, i.e. it is superseded by states of completely different symmetry which correspond to highly-excited states for small U . The situation becomes even more involved for 8 electrons, with small- U ground states becoming large- U excited states, and small- U low-lying excited states mixing with highly excited ones (the $^1\Gamma_1$ symmetry) to contribute to the large- U ground-state manifold.

Figure 4 shows the temperature dependence of the contribution of the various symmetries to the thermodynamic equilibrium state. It is seen there that even though the 2L_3 symmetry -- the one obtained from the Gutzwiller projection -- increases its contribution as T increases, the total spin of the cluster $\langle S(S+1) \rangle$ also increases, making the system more magnetic and therefore less well represented by a projection of a paramagnetic state.

These observations lead one to conclude that the Gutzwiller projection technique alone is inadequate, that one requires in addition the minimization of the Coulomb expectation (2.5), but even so the description of the manifold of ground- and low-lying states is inadequate with the projected states alone.

IV. RESULTS

A. Superconducting correlations

The eight-atom cluster, a finite system, is unable to exhibit the infinite-range correlation behavior of a superconducting transition, i.e. the important region in reciprocal space, the small \vec{k} region, is inaccessible in this treatment, and it is possible that the finiteness might introduce artificial correlations³⁰. However, it has been the belief of the present authors and others⁹, that the study of the fluctuations towards superconductivity in these small systems could yield clues to the real phenomenon. Along those lines, and following the BCS formalism, one has an order parameter $\Delta(\vec{R}, \vec{r})$, which corresponds to the system forming Cooper pairs, of the form :

$$\Delta(\vec{R}, \vec{r}) = \langle \hat{\Delta}(\vec{R}, \vec{r}) \rangle = \langle \Psi(\vec{R} + \vec{r}/2) \Psi(\vec{R} - \vec{r}/2) \rangle, \quad (4.1)$$

where the system has a pair of normal electrons destroyed, with center of mass \vec{R} and separation \vec{r} . Following Hirsch³¹, one may describe the correlation between the two electrons taking place by one of several modes, the usual on-site ($\vec{r} = 0$) spin-singlet coupling (SP) of the form :

$$c_{i\uparrow} c_{i\downarrow}, \quad (4.2)$$

an extended-singlet pairing (SPX) :

$$c_{i\uparrow} c_{i+r\downarrow} - c_{i\downarrow} c_{i+r\uparrow}, \quad (4.3)$$

and a (necessarily) extended spin-triplet pairing, as in liquid He³, with components referred to as TP \uparrow (triplet parallel, $S_z = 1$), TP0 (antiparallel, $S_z = 0$), and TP \downarrow ($S_z = -1$) of forms :

$$c_{i\uparrow} c_{i+r\uparrow}, \quad (4.4)$$

$$c_{i\uparrow} c_{i+r\downarrow} + c_{i\downarrow} c_{i+r\uparrow}, \quad (4.5)$$

$$c_{i\downarrow} c_{i+r\downarrow}, \quad (4.6)$$

respectively. In uniform systems the position \vec{R} within the crystal has no intrinsic importance³². One may proceed directly to reciprocal \vec{k} -space via Fourier transform:

$$\Delta(\vec{k}, \vec{r}) = \frac{1}{\Omega} \int e^{i\vec{k} \cdot \vec{R}} \Delta(\vec{R}, \vec{r}) d^3R; \quad (4.7)$$

In finite systems, one may study the order parameter fluctuation,

$$S(\vec{k}, \vec{r}) = \langle \hat{\Delta}(\vec{k}, \vec{r}) \hat{\Delta}^\dagger(\vec{k}, \vec{r}) \rangle, \quad (4.8)$$

which may be considered as a susceptibility to Cooper pair formation, i.e. the amount of phase space

available to such a possible condensation process. The dependence on \vec{r} yields information on the spatial distribution of the correlation; the \vec{k} -dependence yields the transport and coherence properties. As the object $S(\vec{k}, \vec{r})$ is related quadratically to the order parameter, one may not speak of the spatial distribution of superconducting correlations, but only of the square. Thus triplet-spin pairings, which necessitate odd-parity (p , f , etc.) spatial wavefunctions, would have (s , d , etc.) even-parity $S(\vec{k}, \vec{r})$ distributions, as do singlet pairings.

In the present context, with an eight-atom crystal, there are correspondingly 8 \vec{k} -vectors in the Brillouin Zone, one at Γ (written as γ), three at X (x_1, x_2, x_3), and four at L (l_1, l_2, l_3, l_4). It can be shown then that the SPX and TP0 correlations, written in the k -basis $a_{\kappa\sigma}$, take the forms:

$$\hat{S}_{SPX/TP0}(k, r) = \frac{2}{N} (1 \pm e^{ik \cdot r}) [N - n + \sum_{\kappa_1, \kappa_2} e^{i(\kappa_1 - \kappa_2) \cdot r} a_{\kappa_2 \uparrow}^\dagger a_{\kappa_1 \uparrow} a_{\kappa_2 + k \downarrow}^\dagger a_{\kappa_1 + k \downarrow}]. \quad (4.9)$$

One can immediately see that the pre-factor $(1 \pm e^{ik \cdot r})$ forces the correlations of these two forms to take on non-zero values in complementary parts of k -space, as the exponential term for this cluster takes on only values ± 1 . Similarly, one can establish the expressions for the parallel triplet forms :

$$\hat{S}_{TP\sigma}(k, r) = \frac{1}{2N} (1 - e^{ik \cdot r}) [2N - 3n_\sigma + \sum_{\kappa_1, \kappa_2} e^{i(\kappa_1 - \kappa_2) \cdot r} a_{\kappa_2 \sigma}^\dagger a_{\kappa_1 \sigma} a_{\kappa_2 + k \sigma}^\dagger a_{\kappa_1 + k \sigma}], \quad (4.10)$$

where n_σ refers to the number of electrons aligned with σ . There are six distinct first-nearest neighbors in this model (each represented twice, to give the 12 nearest neighbors of the fcc structure) and thus the information provided by the six $S(k, r=\tau_1, \tau_2, \tau_3, \tau_5, \tau_6, \tau_7)$, where the τ_i 's represent the associated displacement vectors, is just sufficient to expand unambiguously the spatial dependence in terms of the s and the five d functions $zx, yz, xy, x^2 - y^2$ and $3z^2 - r^2$. Within a normalization factor of $[(2l+1)/4\pi]^{1/2}$, the expansion coefficients can be given as :

$$A_s(k) = \frac{1}{6} [S(k, \tau_1) + S(k, \tau_2) + S(k, \tau_3) + S(k, \tau_5) + S(k, \tau_6) + S(k, \tau_7)] \quad (4.11)$$

$$A_{xx}(k) = \frac{1}{\sqrt{3}} [S(k, \tau_1) - S(k, \tau_5)] \quad (4.12)$$

$$A_{yz}(k) = \frac{1}{\sqrt{3}} [S(k, \tau_2) - S(k, \tau_6)] \quad (4.13)$$

$$A_{xy}(k) = \frac{1}{\sqrt{3}} [S(k, \tau_3) - S(k, \tau_7)] \quad (4.14)$$

$$A_{x^2 - y^2}(k) = \frac{1}{\sqrt{3}} [(S(k, \tau_1) + S(k, \tau_5)) - (S(k, \tau_2) + S(k, \tau_6))] \quad (4.15)$$

$$A_{3z^2-r^2}(k) = \frac{1}{3}[S(k, \tau_1) + S(k, \tau_2) - 2S(k, \tau_3) + S(k, \tau_5) + S(k, \tau_6) - 2S(k, \tau_7)] \quad (4.16)$$

For an occupation of 7 electrons the true heavy-fermion ground-state manifold -- comprising the symmetries ${}^2\Gamma_2$, 2X_1 and 2X_2 -- and the low-lying excited states of symmetry 2L_3 , are allowed to mix by (4.9) or (4.10), and the patterns of mixing are presented in Tables II and IV, with the actual values of the correlation matrices presented in Tables III and V, respectively. Thus, any trends towards the symmetry-breaking of a superconducting transition can be detected.

Qualitatively, the first thing to note is that the excited 2L_3 states do not mix with any of the ground-states symmetries for any of the spin-coupling modes. The only mixing occurs between each of the three pairs of 2X_1 and 2X_2 .

Quantitative results are given in Table VI. Here all correlation strengths are normalized to one, i.e. divided by the maximal eigenvalue over all possible 11440 states. For SPX coupling one notices a considerable enhancement from the almost non-interacting to the Gutzwiller-projected state, but the enhancement from the latter to the true ground state -- of different symmetry -- is approximately the same; in other words, the difference between the non-interacting and true states is twice as large as the Gutzwiller method would yield. One sees the same trend, albeit more weakly, for the triplet TP0 and TP \uparrow modes. They both favor a broken-symmetry state. Because these correlations were calculated for the $S_z = +1/2$ states -- four electrons with spin up, three electrons with spin down -- the TP \downarrow mode is strongly disfavored, as seen also in Table VI.

The evidence appears to favor, in the large- U limit, the extended-singlet over the triplet pairings, a result noted before in the literature^{31,33}. However, the critical result here is that *the Gutzwiller-projected state, has neither the correlation strength of the true ground state, nor in any way participates with the ground state to break symmetry and lead towards Cooper pair formation.*

Having decided on the 2X_1 state in the SPX coupling mode as the leading superconducting candidate, one can now apply (4.11-16) to describe its s - d -decomposition, the results of which are presented in Table VII. One can see quite clearly the degree of anisotropy, both in real and in k -space.

B. BCS wavefunction for a finite cluster

In 1957, Bardeen, Cooper and Schrieffer wrote their celebrated paper³⁴ describing the superconducting-state function:

$$|\Psi_{BCS}\rangle = \prod_{\vec{k}} (u_{\vec{k}} + v_{\vec{k}} a_{\vec{k}\uparrow}^{\dagger} a_{-\vec{k}\downarrow}^{\dagger}) |0\rangle, \quad (4.17)$$

where the coefficients $u_{\vec{k}}$ and $v_{\vec{k}}$ are expressed as³⁵:

$$u_{\vec{k}}^2 = \frac{1}{2} [1 + \epsilon_{\vec{k}} / (e_{\vec{k}}^2 + \Delta_{\vec{k}}^2)^{1/2}] \quad (4.18)$$

$$v_{\vec{k}}^2 = \frac{1}{2} [1 - \epsilon_{\vec{k}} / (e_{\vec{k}}^2 + \Delta_{\vec{k}}^2)^{1/2}] \quad (4.19)$$

Here $\epsilon_{\vec{k}}$ refers to the one-electron energy of \vec{k} , measured from the Fermi energy, whereas $\Delta_{\vec{k}}$ represents the corresponding superconducting energy-gap parameter. Historically, the fears that the BCS equation (4.17) (i) did not conserve the number of particles, and (ii) in the thermodynamic limit the predicted wave function was orthogonal to the true ground state, were eventually resolved and the approach has become the cornerstone of the theory of superconductivity.

Recently Gros³⁶ has examined the consequence of projecting the BCS-state onto a fixed number of electrons in a finite cluster, and then applying the Gutzwiller projection to remove any doubly-occupied states. This approach has the advantage of allowing the system in question to reveal its own preferred coupling mode, rather than attempting to match the correlation to those of given models.

In the present situation, given the advantage of considering an even number of electrons, it is convenient to choose the eight-site cluster with six electrons. Thus, the wavefunction of (4.17) would take on the (unnormalized) form:

$$|\Psi_{BCS}\rangle = \sum_{\kappa_0, \dots, \kappa_7} v_{\kappa_0} v_{\kappa_1} v_{\kappa_2} u_{\kappa_3} u_{\kappa_4} u_{\kappa_5} u_{\kappa_6} u_{\kappa_7} a_{\kappa_0\uparrow}^{\dagger} a_{\kappa_0\downarrow}^{\dagger} a_{\kappa_1\uparrow}^{\dagger} a_{\kappa_1\downarrow}^{\dagger} a_{\kappa_2\uparrow}^{\dagger} a_{\kappa_2\downarrow}^{\dagger} |0\rangle, \quad (4.20)$$

where κ_0, κ_1 and κ_2 are the occupied electron-pair states and κ_3 through κ_7 are the empty one-electron states. Equation (4.20) is considered here in two limits: the almost-non-interacting (small U) and the Gutzwiller-projected strongly-interacting (large U) extremes. For $U = 0$, there are 56 states corresponding to occupied triplets of k -pairs (3 chosen from 8), while in the infinite- U limit, the Gutzwiller projection (2.6) reduces these to 28 possible states.

For U vanishingly small, if one restricts the choices for the triplets of occupied k -pairs to the γ -pair, and two of the four l -pairs, then one obtains directly a state with energy contributions from (2.3) and (2.4) of $(-24t + 12T)$, which corresponds to the vanishing- U ground state. This is equivalent to setting

$$v_\gamma = u_{x_1} = u_{x_2} = u_{x_3} = 1, u_\gamma = v_{x_1} = v_{x_2} = v_{x_3} = 0 \quad (4.21)$$

which amounts to setting the energy-gap parameters, $\Delta_\gamma = \Delta_{x_i} = 0$. This leaves the four (u_l, v_l) pairs free to reduce the Coulomb energy (2.5).

Without the constraint of the BCS variational wavefunction, the six functions, denoted by the $(\vec{k}\uparrow, \vec{k}\downarrow)$ pairings $\gamma l_1 l_2$, $\gamma l_1 l_3$, $\gamma l_1 l_4$, $\gamma l_2 l_3$, $\gamma l_2 l_4$, and $\gamma l_3 l_4$, form representations of $^1\Gamma_1$, $^1\Gamma_{12}$ and $^1\Gamma'_{15}$, with expectations, $13U/8$, $7U/8$ and $9U/8$, respectively. It should be noted that the $^1\Gamma_1$ and $^1\Gamma'_{15}$ states correspond exactly to those listed among the low-lying states in Table I, while the $^1\Gamma_{12}$ state overlaps only partially the true ground state.

It can be shown that the Coulomb energy expectation value, with the BCS state, is

$$\langle H_C \rangle = U [1 + 1/8[(\sum_p v_p u_r u_s)^2 - 6u_{l_1} v_{l_1} u_{l_2} v_{l_2} u_{l_3} v_{l_3} u_{l_4} v_{l_4}]/\sum_p v_p^2 u_r^2 u_s^2]], \quad (4.22)$$

where the summations are over the four l -states. This is not a simple problem in optimization. However, one can argue, by symmetry, that the optimum solutions will lie on loci of high symmetry. If, for example, one sets all the u 's and v 's constant, which would amount to s -wave pairing, one obtains precisely the $^1\Gamma_1$ state. Thus, if one were to use the BCS wavefunction for attractive potentials, where $U < 0$, one would obtain the correct ground state.

To obtain the minimum of (4.22) for $U > 0$, if one calls this minimum yU , sets any two pairs of the (u_i, v_i) 's equal (three such combinations, e.g. $u_{l_1} = u_{l_3} = u_1$, $u_{l_2} = u_{l_4} = u_2$, and similarly for the v 's), and introduces a variable $x = u_1 v_2 / u_2 v_1$, one obtains :

$$(1 + x^4)(8y - 9) - 8(x^3 + x) + x^2(32y - 44) = 0. \quad (4.23)$$

Upon minimization with respect to y (4.23) yields an extremum with the unusual value

$$y = (17\sqrt{3} - 39)/(8\sqrt{3} - 24) = 0.941987298 \quad (4.24)$$

which is achieved for

$$x = \pm(\sqrt{3}/2)^{1/2} - (1 + \sqrt{3}/2)^{1/2} = (-2.296630), \quad (-0.435420) \quad (4.25)$$

Clearly, this solution is a compromise. Although it minimizes the band energy, it does not reach the minimum $7U/8$ Coulomb energy accessible with the full BCS set (4.20). And in fact it represents only a 59.15% overlap with the true Γ_{12} ground-state, of expectation $3U/4$.

For infinite U , the one-electron orbital energies cease to have meaning. However, if one seeks a solution with minimal nearest-neighbor band energy (2.2), then one finds a minimal manifold corresponding to the choices for (u_i, v_i) of (4.21). Without further BCS constraints, this manifold has expectation values for (2.2) of $(-32t/5)$, $(-96t/11)$ and $(-272t/23)$ [equal to $(-6.4t)$, $(-8.727t)$, $(-11.826t)$, respectively] corresponding respectively to the symmetries $^1\Gamma_1$, $^1\Gamma_{25'}$ and $^1\Gamma_{12}$. This results compares with the true ground-state energy of $(-12t)$. The minimization problem becomes somewhat more complicated than for infinitesimal U , of the form :

$$\begin{aligned} \langle H_{1m} \rangle = & -8t [23 \sum v_p^2 v_q^2 u_r^2 u_s^2 - 5(\sum v_p v_q u_r u_s)^2 + 66u_1 v_1 u_2 v_2 u_3 v_3 u_4 v_4] / \\ & [17 \sum v_p^2 v_q^2 u_r^2 u_s^2 - 3(\sum v_p v_q u_r u_s)^2 + 36u_1 v_1 u_2 v_2 u_3 v_3 u_4 v_4] \end{aligned} \quad (4.26)$$

Again, as in the infinitesimal- U limit, the maximum $^1\Gamma_1$ value may be achieved in an s-wave pairing. The minimal value possible, however, achieved for $x = u_1 v_2 / u_2 v_1 = -1$, is $(-736t/63)$ [equal to $(-11.683t)$].

To study the superconducting energy-gap parameters, one may expand their distributions, as a function of k , in terms of functions following the symmetries s , d , etc. [even parity only is considered with the singlet-spin mode of (4.17)]. With eight k -vectors in this small cluster, one has a basis of 8 k -functions to work with, and one can obtain, as Sigrist and Rice do³⁷ for the high- T_c square lattice, the functions compatible with the lattice. For the energy-gap parameters among the l 's, this amounts to the following contributions of d -functions:

$$d_{xy} = \Delta_{l_1} - \Delta_{l_2} - \Delta_{l_3} + \Delta_{l_4}, \quad (4.27)$$

$$d_{yz} = \Delta_{l_1} + \Delta_{l_2} - \Delta_{l_3} - \Delta_{l_4}, \quad (4.28)$$

$$d_{zx} = \Delta_{l_1} - \Delta_{l_2} + \Delta_{l_3} - \Delta_{l_4}, \quad (4.29)$$

and in addition the s -like function

$$s = \Delta_{l_1} + \Delta_{l_2} + \Delta_{l_3} + \Delta_{l_4}. \quad (4.30)$$

Thus, one sees a definite d -character for the BCS state. However, it is an unsatisfactory approximation, in both low- and high- U limits: the expectation values of the total energy are not close to the true ground-state energy.

C. Magnetic correlations

As the fcc structure is composed of triangular rings of bonds, the antiferromagnetic coupling (2.4) is frustrated in its attempt to saturate the system. Thus the interaction of the band structure with the spin geometry, a possible resolution of the RVB proposal, is of great interest. In this cluster, there are three reasonable spin-spin correlations to examine -- on-site, first and second neighbors -- of forms

$$L_0 = \frac{1}{N} \sum_i S_{iz}^2, \quad (4.31)$$

$$L_1 = \frac{1}{N} \sum_{\langle ij \rangle 1nn} S_{iz} S_{jz}, \quad (4.32)$$

$$L_2 = \frac{1}{N} \sum_{\langle ij \rangle 2nn} S_{iz} S_{jz}, \quad (4.33)$$

respectively, N being the number of sites. It should be pointed out that, within the eight-atom cluster, a sum rule exists,

$$L_0 + 2L_1 + 2L_2 = S_z^2/16, \quad (4.34)$$

where S_z is the z -projection of the spin. Furthermore, in the infinite- U limit, one has L_0 tending upwardly to $n/4N$, where n is the number of electrons.

The results for the ground- and low-lying states for 6,7 and 8 electrons in the small and high U limits are presented in Table VIII, along with the extreme values possible for each configuration.

Very clear trends can be gathered from the table. First, at both the low- and high- U limits, the ground state is most strongly nearest-neighbor antiferromagnetic, with L_1 increasing monotonically with excitation energy. The exact opposite can be said of the second-nearest-neighbor behavior. Also, as a function of U , one sees that L_0 and L_2 increase, and L_1 decreases.

Thus, the tendencies at both extremes is towards antiferromagnetism, and states which at low- U may be the ground states, may find themselves overtaken, at high- U , by completely different electronic configurations which are more antiferromagnetic.

IV. CONCLUSIONS

A model for superconducting and magnetic behavior in a heavy-fermion system, one comprising an eight-atom cluster in the fcc structure with occupancies of 6, 7 and 8 electrons, was examined. A critique of ongoing work is obtained. Although too small a cluster to observe the important long-range correlations present in superconducting transitions, it is the opinion of the authors that this smallness, allowing a full description of the model system, more than makes up for this liability, while other approaches, such as Monte Carlo^{9,36} may be leaving subtle gaps in the true picture.

It was observed that the Gutzwiller projection²⁶, which obtains a heavy-fermion wavefunction from the non-interacting function by projecting out any part containing any doubly-occupied atoms, is an inadequate description of the ground state and low-lying excitations. This inadequacy becomes more pronounced as one nears the half-filled limit, which is where all the interesting heavy-fermion behavior occurs. The amendment to the projection proposed here, that is, *to take the linear combination of non-interacting ground state wavefunctions which minimizes the Coulomb repulsion*, acts to achieve the optimum state from within that restricted manifold.

The model demonstrates a trend towards superconductivity which is of extended-spin-singlet form and highly anisotropic, with significant *s*- and *d*-wave mixing. No significant trends towards symmetry-breaking was noted, indicating possibly that the large-*U* Hubbard mechanism is not, of itself, responsible for superconductivity; rather, it might be said that, at best, it makes phase space available for another mechanism, such as the standard phonon coupling, to allow superconductivity to proceed. In light of recent evidence denying any magnetic activity in the Yttrium compounds³⁸, this may be an optimistic assessment.

The BCS trial state, restricted to the small cluster, describes states of considerable *d*-character, and was shown to be inadequate both in the small and large *U* regimes, removed considerably from the true ground state. For small attractive *U*, however, the BCS wavefunction corresponded exactly to the true ground state.

The magnetic correlations showed that this model is remarkably good for antiferromagnetic behavior, with strong antiferromagnetic ordering in both the small and large *U* limits.

The authors recognize that many of the condemnations of the Gutzwiller projection process may be due to finite-size effects³⁰. It is possible that the projection process, applied to increasingly larger clusters, may approach a total description of the ground-state behavior, but this is a conjecture which should be scrupulously examined. The present approach, as detailed in previous work²⁰, does not scale well, so the question may remain open for some time to come.

ACKNOWLEDGMENTS

The authors wish to thank Cesar Proetto for lively and stimulating discussions. This research was supported, in part, at the Lawrence Berkeley Laboratory by the Director, Office of Energy Research, Office of Basic Energy Sciences, Materials Sciences Division, U.S. Department of Energy, under contract No. DE-AC03-76SF00098. The authors also wish to acknowledge the gracious hospitality, in Copenhagen, of the Nordisk Institut for Teoretisk Atomfysik (NORDITA), and of the H. C. Ørsted Institutet.

REFERENCES

- 1 G.R. Stewart, Rev. Mod. Phys. **56** , 755 (1984).
- 2 F. Steglich, in *Theory of Heavy Fermions and Valence Fluctuations*, edited by K. Kasuya and T. Saso, Springer Series in Solid State Sciences, Vol. 62 (Springer, New York, 1985), p.23.
- 3 W. Buckel and W. Weber, *Superconductivity in d- and f-Band Metals 1982*, (Kenforschungszentrum Karlsruhe GmbH, Karlsruhe, 1982).
- 4 H. Suhl and M.B. Maple, *Superconductivity in d- and f-Band Metals*, (Academic Press, New York, 1980).
- 5 T.M. Rice, Z. Phys. B. **67** , 141 (1987).
- 6 C. Gros, R. Joynt and T.M. Rice, Phys. Rev. B. **36** , 381 (1987).
- 7 P. Fulde, J. Keller and G. Zwicknagl, *Theory of Heavy Fermion Systems*,
- 8 J.E. Hirsch, Phys. Rev. Lett. **59** , 228 (1987). (Max Planck Inst., Stuttgart), 1987.
- 9 C. Gros, R. Joynt and T.M. Rice, Z. Phys. B. **68** , 425 (1987).
- 10 J. Hubbard, Proc. R. Soc. London, Ser A **276** , 238 (1963); **277** , 237 (1964); **281** , 401 (1964); **285** , 542 (1965); **296** , 82 (1966); **296** , 100 (1967).
- 11 P.W. Anderson, Phys. Rev., **124** , 41 (1961).
- 12 R.H. Victora and L.M. Falicov, Phys. Rev. B **30** , 1695 (1984).
- 13 R.H. Victora and L.M. Falicov, Phys. Rev. Lett. **55** , 1140 (1985).
- 14 A. Reich and L.M. Falicov, Phys. Rev. B **34** , 6752 (1986).
- 15 J.C. Parlebas, R.H. Victora, and L.M. Falicov, J. Phys. (Paris) **47** , 1029 (1986).
- 16 E.C. Sowa and L.M. Falicov, Phys. Rev. B **35** , 3765 (1987).
- 17 J. Callaway, D.P. Chen and R. Tang, Z. Phys. D **3** , 91 (1986); Phys. Rev. B. **35** , 3705 (1987).
- 18 J. Callaway, Phys. Rev. B. **35** , 8723 (1987).
- 19 A. Reich and L.M. Falicov, Phys. Rev. B. **36** , 3117 (1987).

- 20 A. Reich and L.M. Falicov, Phys. Rev. B **37** , [to appear] (1988).
- 21 P.W. Anderson, Science **235** , 1196 (1987).
- 22 P.W. Anderson, in *Solid State Physics*, edited by F.Seitz and D. Turnbull, (Academic Press, New York, 1963) Vol. 14, p.99.
- 23 A.B. Harris and R.V. Lange, Phys. Rev. **157** , 295 (1967).
- 24 J.R. Schrieffer and P.A. Wolff, Phys. Rev. **149** , 491 (1966).
- 25 L. P. Bouckaert, R. Smoluchowsky and E. Wigner, Phys. Rev. **50** , 58 (1936).
- 26 M.C. Gutzwiller, Phys. Rev. A. **137** , 1726 (1965).
- 27 P. Coleman, Phys. Rev. B. **29** , 3035 (1984).
- 28 C.S. Wang, M.R. Norman, R.C. Albers, A.M.Boring, W.E. Pickett, H. Krakauer, and N.E. Christensen, Phys. Rev. B. **35** , 7260 (1987).
- 29 F. Gebhard and D. Vollhardt, Phys. Rev. Lett. **59** , 1472 (1987).
- 30 G. Stollhoff, Z. Phys. B. **69** , 61 (1987).
- 31 J.E. Hirsch, Phys. Rev. Lett. **54** , 1317 (1985).
- 32 It should be remembered that the \vec{R} dependence, which enters explicitly into the Landau-Ginzburg equations, is used to describe vortices, magnetic impurities, surfaces, interfaces, and other features on the scale of the correlation length, clearly outside the reach of the present treatment.
- 33 D.J. Scalapino, E. Loh, Jr. and J.E. Hirsch, Phys. Rev. B. **34** , 8190 (1986).
- 34 J. Bardeen, L.N. Cooper and J.R. Schrieffer, Phys. Rev. **108** , 1175 (1957).
- 35 C. Kittel, *Quantum Theory of Solids*, (Wiley, New York, 1963), p. 166.
- 36 C. Gros, private communication.
- 37 M. Sigrist and T.M. Rice, Z.Phys.B. **68** , 9 (1987).
- 38 T. Bruckel, H. Capellmann, W. Just, O. Scharpf, S. Kemmler-Sack, R. Kiemel and W. Schaefer, Europhys. Lett. **4** , 1189 (1987).

FIGURE CAPTIONS

- 1 Schematic representation of the ground- and low-lying states for 6 electrons. The situation is rather straightforward: the symmetries at low- U carry over to the high- U regime, with no cross-overs.
- 2 Schematic representation of the ground- and low-lying states for 7 electrons. Here, the low- U ground states form high- U excited states, with completely different symmetries crossing over.
- 3 Schematic representation of the ground- and low-lying states for 8 electrons. The trend as for 7 electrons continues, with many cross-overs, showing the Gutzwiller-projected states to be an inadequate description of the spectrum.
- 4 The competing effects of superconductivity and magnetism are most aptly demonstrated by comparing the thermal probability behavior of the seven-electron superconducting candidate, 2X_1 , with the Gutzwiller-projected state 2L_3 , and the mean-spin-squared $\langle S(S+1) \rangle$. The two states do not mix to form a broken-symmetry superconducting complex, the 2X_1 has a stronger correlation than the 2L_3 , and the latter is washed out by an increasing ferromagnetic tendency.

TABLES

TABLE I.

Many-body energies of the low-lying states for 6, 7, and 8 electrons in the infinitesimal and infinite- U limits.

small U			large U		
Energy	States	Symmetries	Energy	States	Symmetries
6 electrons					
$-24t + 12T + 5U/8$	16	$^1\Gamma_{12}, ^3X_2, ^5\Gamma_2$	$-12t + 12T - 11J/4$	2	$^1\Gamma_{12}$
$-24t + 12T + 9U/8$	57	$^1\Gamma'_{25}, ^1X_3, ^1X_5, ^3\Gamma'_{15}, ^3X_2, ^3X_4, ^3X_5$	$-12t + 12T - 7J/4$	9	3X_2
$-24t + 12T + 13U/8$	6	$^1\Gamma_1, ^1\Gamma_{12}, ^1X_1$	$-12t + 12T + J/4$	5	$^5\Gamma_2$
7 electrons					
$-24t + 18T + 5U/4$	32	$^2L_3, ^4L_2$	$-6t + 6T - 3J$	14	$^2\Gamma_2, ^2X_1, ^2X_2$
$-24t + 18T + 7U/4$	24	$^2L_2, ^2L_3$	$-6t + 6T - 2J$	16	2L_3
			$-6t + 6T - 3J/2$	32	$^4\Gamma_{12}, ^4X_1, ^4X_2$
			$-6t + 6T - J/2$	16	4L_2
			$-6t + 6T + J$	18	6X_2
8 electrons					
$-24t + 24T + 15U/8$	24	$^1\Gamma'_{25}, ^1X_3, ^3X_5$	$-4J$	3	$^1\Gamma_1, ^1\Gamma_{12}$
$-24t + 24T + 19U/8$	4	$^1\Gamma_1, ^1X_1$	$-3J$	22	$^1L_2, ^3X_1, ^3X_2$
			$-2J$	42	$^1\Gamma'_{25}, ^1X_3, ^3L_2, ^3L_3$
			$-J$	48	$^3X_5, ^5\Gamma_1, ^5\Gamma_{12}, ^5X_1$
			0	53	$^1\Gamma_1, ^3L_2, ^5L_3$
			J	30	$^5\Gamma'_{25}, ^5X_3$
			$2J$	21	7X_1
			$3J$	28	7L_1
			$6J$	9	$^9\Gamma_1$

TABLE II.

Correlation mixing pattern for 7-electron heavy-fermion ground-state manifold

		singlet pairing								triplet pairing							
state(s)		γ	x_1	x_2	x_3	l_1	l_2	l_3	l_4	x_1	x_2	x_3	l_1	l_2	l_3	l_4	
τ_1	$ ^2\Gamma_2\rangle$	r	r					r	r	r	r		r	r			
	$ ^2X_1(a)\rangle ^2X_2(a)\rangle$	A_0	A_0					A_0	A_0	A_0	A_0		A_0	A_0			
	$ ^2X_1(b)\rangle ^2X_2(b)\rangle$	B_+	B_+					B_+	B_+	B_-	B_-		B_-	B_-			
	$ ^2X_1(c)\rangle ^2X_2(c)\rangle$	B_-	B_-					B_-	B_-	B_+	B_+		B_+	B_+			
τ_2	$ ^2\Gamma_2\rangle$	r		r			r		r	r		r			r		
	$ ^2X_1(a)\rangle ^2X_2(a)\rangle$	B_-		B_-			B_-		B_-	B_+		B_+			B_+		
	$ ^2X_1(b)\rangle ^2X_2(b)\rangle$	A_0		A_0			A_0		A_0	A_0		A_0			A_0		
	$ ^2X_1(c)\rangle ^2X_2(c)\rangle$	B_+		B_+			B_+		B_+	B_-		B_-			B_-		
τ_3	$ ^2\Gamma_2\rangle$	r			r		r		r	r		r				r	
	$ ^2X_1(a)\rangle ^2X_2(a)\rangle$	B_+			B_+		B_+		B_+	B_-		B_-			B_-		
	$ ^2X_1(b)\rangle ^2X_2(b)\rangle$	B_-			B_-		B_-		B_-	B_+		B_+			B_+		
	$ ^2X_1(c)\rangle ^2X_2(c)\rangle$	A_0			A_0		A_0		A_0	A_0		A_0			A_0		
τ_5	$ ^2\Gamma_2\rangle$	r	r				r		r		r				r	r	
	$ ^2X_1(a)\rangle ^2X_2(a)\rangle$	A_0	A_0				A_0		A_0	A_0	A_0				A_0	A_0	
	$ ^2X_1(b)\rangle ^2X_2(b)\rangle$	B_+	B_+				B_+		B_+	B_-	B_-				B_-	B_-	
	$ ^2X_1(c)\rangle ^2X_2(c)\rangle$	B_-	B_-				B_-		B_-	B_+	B_+				B_+	B_+	
τ_6	$ ^2\Gamma_2\rangle$	r		r			r		r	r		r			r		
	$ ^2X_1(a)\rangle ^2X_2(a)\rangle$	B_-		B_-			B_-		B_-	B_+		B_+			B_+	B_+	
	$ ^2X_1(b)\rangle ^2X_2(b)\rangle$	A_0		A_0			A_0		A_0	A_0		A_0			A_0	A_0	
	$ ^2X_1(c)\rangle ^2X_2(c)\rangle$	B_+		B_+			B_+		B_+	B_-		B_-			B_-	B_-	
τ_7	$ ^2\Gamma_2\rangle$	r			r		r		r	r		r			r		
	$ ^2X_1(a)\rangle ^2X_2(a)\rangle$	B_+			B_+		B_+		B_+	B_-		B_-			B_-	B_-	
	$ ^2X_1(b)\rangle ^2X_2(b)\rangle$	B_-			B_-		B_-		B_-	B_+		B_+			B_+	B_+	
	$ ^2X_1(c)\rangle ^2X_2(c)\rangle$	A_0			A_0		A_0		A_0	A_0		A_0			A_0	A_0	

TABLE III.

Values for the couplings of the heavy-fermion ground-state manifold for 7 electrons

coupling	r	A_0	B_{\pm}
SPX	7/4	$\begin{bmatrix} 11/4 & 0 \\ 0 & 19/12 \end{bmatrix}$	$\begin{bmatrix} 5/4 & \pm 7\sqrt{2}/12 \\ \pm 7\sqrt{2}/12 & 11/6 \end{bmatrix}$
TP0	13/12	$\begin{bmatrix} 3/4 & 0 \\ 0 & 41/36 \end{bmatrix}$	$\begin{bmatrix} 5/4 & \pm 7\sqrt{2}/36 \\ \pm 7\sqrt{2}/36 & 19/18 \end{bmatrix}$
TP \uparrow	1/6	$\begin{bmatrix} 1/6 & 0 \\ 0 & 13/36 \end{bmatrix}$	$\begin{bmatrix} 1/2 & \pm \sqrt{2}/9 \\ \pm \sqrt{2}/9 & 5/12 \end{bmatrix}$
TP \downarrow	7/12	$\begin{bmatrix} 7/12 & 0 \\ 0 & 7/9 \end{bmatrix}$	$\begin{bmatrix} 3/4 & \pm \sqrt{2}/12 \\ \pm \sqrt{2}/12 & 23/36 \end{bmatrix}$

TABLE IV.

Correlation mixing pattern for the 7-electron Gutzwiller state manifold in the large U limit

	singlet pairing								triplet pairing							
state(s)	γ	x_1	x_2	x_3	l_1	l_2	l_3	l_4	x_1	x_2	x_3	l_1	l_2	l_3	l_4	
τ_1																
$ ^2L_3(1)\rangle ^2L_3(2)\rangle$	A_0	A_0					A_0	A_0		A_0	A_0	A_0	A_0			
$ ^2L_3(3)\rangle ^2L_3(4)\rangle$	A_0	A_0					A_0	A_0		A_0	A_0	A_0	A_0			
$ ^2L_3(5)\rangle ^2L_3(6)\rangle$	B_-	B_-					B_-	B_-		B_+	B_+	B_+	B_+			
$ ^2L_3(7)\rangle ^2L_3(8)\rangle$	B_-	B_-					B_-	B_-		B_+	B_+	B_+	B_+			
τ_2																
$ ^2L_3(1)\rangle ^2L_3(2)\rangle$	A_+		A_+			A_+		A_+	A_-		A_-	A_-		A_-		
$ ^2L_3(3)\rangle ^2L_3(4)\rangle$	B_-		B_-			B_-		B_-	B_+		B_+	B_+		B_+		
$ ^2L_3(5)\rangle ^2L_3(6)\rangle$	A_0		A_0			A_0		A_0	A_0		A_0	A_0		A_0		
$ ^2L_3(7)\rangle ^2L_3(8)\rangle$	B_+		B_+			B_+		B_+	B_-		B_-	B_-		B_-		
τ_3																
$ ^2L_3(1)\rangle ^2L_3(2)\rangle$	A_-			A_-		A_-	A_-		A_+	A_+		A_+				A_+
$ ^2L_3(3)\rangle ^2L_3(4)\rangle$	B_+			B_+		B_+	B_+		B_-	B_-		B_-				B_-
$ ^2L_3(5)\rangle ^2L_3(6)\rangle$	B_+			B_+		B_+	B_+		B_-	B_-		B_-				B_-
$ ^2L_3(7)\rangle ^2L_3(8)\rangle$	A_0			A_0		A_0	A_0		A_0	A_0		A_0				A_0
τ_5																
$ ^2L_3(1)\rangle ^2L_3(2)\rangle$	B_0	B_0			B_0	B_0				B_0	B_0			B_0	B_0	
$ ^2L_3(3)\rangle ^2L_3(4)\rangle$	B_0	B_0			B_0	B_0				B_0	B_0			B_0	B_0	
$ ^2L_3(5)\rangle ^2L_3(6)\rangle$	A_-	A_-			A_-	A_-				A_+	A_+			A_+	A_+	
$ ^2L_3(7)\rangle ^2L_3(8)\rangle$	A_-	A_-			A_-	A_-				A_+	A_+			A_+	A_+	
τ_6																
$ ^2L_3(1)\rangle ^2L_3(2)\rangle$	B_+		B_+		B_+		B_+		B_-		B_-		B_-		B_-	
$ ^2L_3(3)\rangle ^2L_3(4)\rangle$	A_-		A_-		A_-		A_-		A_+		A_+		A_+		A_+	
$ ^2L_3(5)\rangle ^2L_3(6)\rangle$	B_0		B_0		B_0		B_0		B_0		B_0		B_0		B_0	
$ ^2L_3(7)\rangle ^2L_3(8)\rangle$	A_+		A_+		A_+		A_+		A_-		A_-		A_-		A_-	
τ_7																
$ ^2L_3(1)\rangle ^2L_3(2)\rangle$	B_-			B_-	B_-			B_-	B_+	B_+			B_+	B_+		
$ ^2L_3(3)\rangle ^2L_3(4)\rangle$	A_+			A_+	A_+			A_+	A_-	A_-			A_-	A_-		
$ ^2L_3(5)\rangle ^2L_3(6)\rangle$	A_+			A_+	A_+			A_+	A_-	A_-			A_-	A_-		
$ ^2L_3(7)\rangle ^2L_3(8)\rangle$	B_0			B_0	B_0			B_0	B_0	B_0			B_0	B_0		

TABLE V.

Values for the couplings of the heavy-fermion Gutzwiller manifold for 7 electrons

coupling	A_0	A_{\pm}	B_0	B_{\pm}
SPX	$\begin{bmatrix} 9/4 & 0 \\ 0 & 17/20 \end{bmatrix}$	$\begin{bmatrix} 6/5 & \pm 7\sqrt{3}/20 \\ \pm 7\sqrt{3}/20 & 19/10 \end{bmatrix}$	$\begin{bmatrix} 33/20 & 0 \\ 0 & 19/12 \end{bmatrix}$	$\begin{bmatrix} 8/5 & \pm\sqrt{3}/60 \\ \pm\sqrt{3}/60 & 49/30 \end{bmatrix}$
TP0	$\begin{bmatrix} 11/12 & 0 \\ 0 & 83/60 \end{bmatrix}$	$\begin{bmatrix} 19/15 & \pm 7\sqrt{3}/60 \\ \pm 7\sqrt{3}/60 & 31/30 \end{bmatrix}$	$\begin{bmatrix} 67/60 & 0 \\ 0 & 41/36 \end{bmatrix}$	$\begin{bmatrix} 17/15 & \pm\sqrt{3}/180 \\ \pm\sqrt{3}/180 & 101/90 \end{bmatrix}$
TP \uparrow	$\begin{bmatrix} 7/20 & 0 \\ 0 & 19/36 \end{bmatrix}$	$\begin{bmatrix} 29/60 & \pm 2\sqrt{3}/45 \\ \pm 2\sqrt{3}/45 & 71/180 \end{bmatrix}$	$\begin{bmatrix} 9/20 & 0 \\ 0 & 73/180 \end{bmatrix}$	$\begin{bmatrix} 5/12 & +\sqrt{3}/90 \\ +\sqrt{3}/90 & 79/180 \end{bmatrix}$
TP \downarrow	$\begin{bmatrix} 17/30 & 0 \\ 0 & 77/90 \end{bmatrix}$	$\begin{bmatrix} 47/60 & \pm 13\sqrt{3}/180 \\ \pm 13\sqrt{3}/180 & 23/36 \end{bmatrix}$	$\begin{bmatrix} 2/3 & 0 \\ 0 & 11/15 \end{bmatrix}$	$\begin{bmatrix} 43/60 & \pm\sqrt{3}/60 \\ \pm\sqrt{3}/60 & 41/60 \end{bmatrix}$

TABLE VI.

Normalized maximal correlation values for 7-electron states at nearest-neighbor separation.

	all states $t, T, U = 0$	almost non-interacting $U = 0^+$	Gutzwiller state $U = \infty$	Heavy-fermion state $U = \infty$	Atomic limit $t, T = 0, U = \infty$
(# states)	11440	56	28	14	1024
SPX	1.0	0.281 $ ^2L_3\rangle$	0.313 $ ^2L_3\rangle$	0.344 $ ^2X_1\rangle$	0.438
TP0	1.0	0.172	0.173	0.181 $0.816 ^2X_1\rangle - 0.577 ^2X_2\rangle$	0.438
TP \uparrow	1.0	0.167	0.176	0.207 $0.793 ^2X_1\rangle - 0.610 ^2X_2\rangle$	0.667
TP \downarrow	1.0	0.479	0.428	0.412 $0.845 ^2X_1\rangle - 0.536 ^2X_2\rangle$	0.500

TABLE VII.

Unnormalized s and d expansion of correlations for the maximally-correlated $|^2X_1\rangle$ state, polarized in the x -direction. The degree of anisotropy is quite notable.

	γ	x_1	x_2	x_3	l_1	l_2	l_3	l_4
s	1.750	0.917	0.417	0.417	0.875	0.875	0.875	0.875
zx	0	0	0	0	-1.588	-1.588	1.588	1.588
yz	0	0	0	0	-0.722	0.722	-0.722	0.722
xy	0	0	0	0	-0.722	0.722	0.722	-0.722
$x^2 - y^2$	1.732	3.175	-1.443	0	0.866	0.866	0.866	0.866
$3z^2 - r^2$	1.000	1.833	0.833	-1.667	0.500	0.500	0.500	0.500

TABLE VIII.

Magnetic correlations for 6, 7 and 8-electron ground and low-lying minimal-spin states in the low and high U limits

state(s)	small U			state(s)	large U		
	L_0	L_1	L_2		L_0	L_1	L_2
6 electrons							
minima	0.0	-0.1563	-0.0938				
maxima	0.1875	0.4063	0.0938				
$^1\Gamma_{12}$	0.1484	-0.0859	0.0117	$^1\Gamma_{12}$	0.1875	-0.1146	0.0208
$^1\Gamma'_{15}, ^1X_3, ^1X_5$	0.1172	-0.0547	-0.0039				
$^1\Gamma_1, ^1\Gamma_{12}, ^1X_1$	0.0859	0.0234	-0.0195				
7 electrons							
minima	0.0313	-0.1875	-0.0313				
maxima	0.2188	0.5625	0.0938				
2L_3	0.1367	-0.0644	-0.0020	$^2\Gamma_2, ^2X_1, ^2X_2$	0.2188	-0.1250	0.0313
$^2L_2, ^2L_3$	0.1211	-0.0508	-0.0098	2L_3	0.2188	-0.0833	0.0104
8 electrons							
minima	0.0	-0.2500	-0.1250				
maxima	0.2500	0.7500	0.1250				
$^1\Gamma'_{25}, ^1X_3$	0.1328	-0.0547	-0.0117	$^1\Gamma_1, ^1\Gamma_{12}$	0.2500	-0.1667	0.0417
$^1\Gamma_1, ^1X_1$	0.1016	-0.0234	-0.0273	1L_2	0.2500	-0.1250	0.0
				$^1\Gamma'_{25}, ^1X_3$	0.2500	-0.0833	-0.0417

Figure 1.

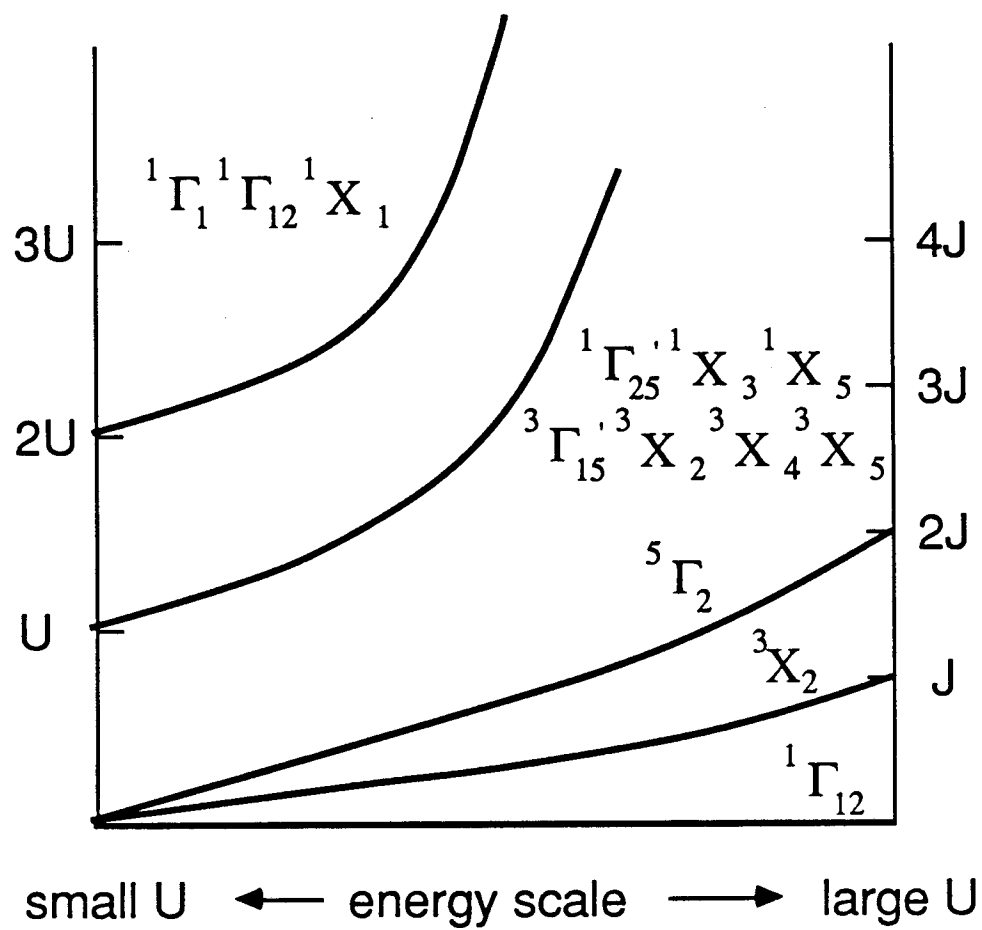


Figure 2.

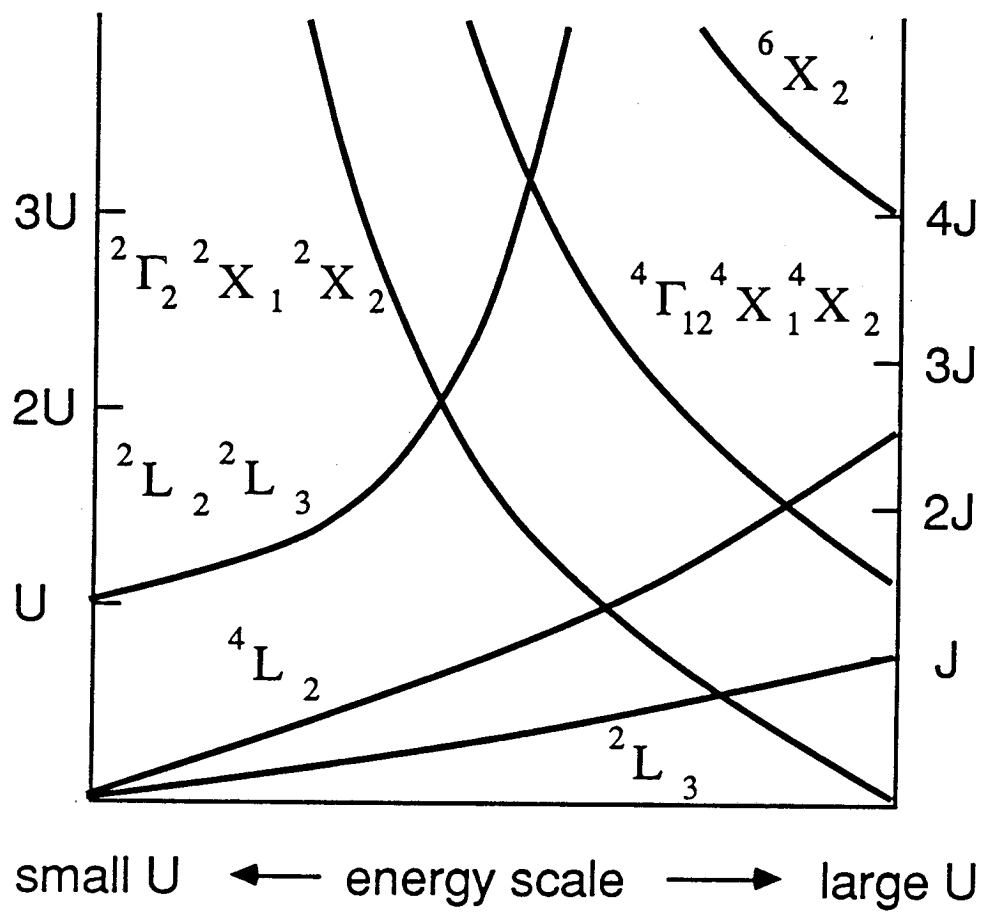


Figure 3.

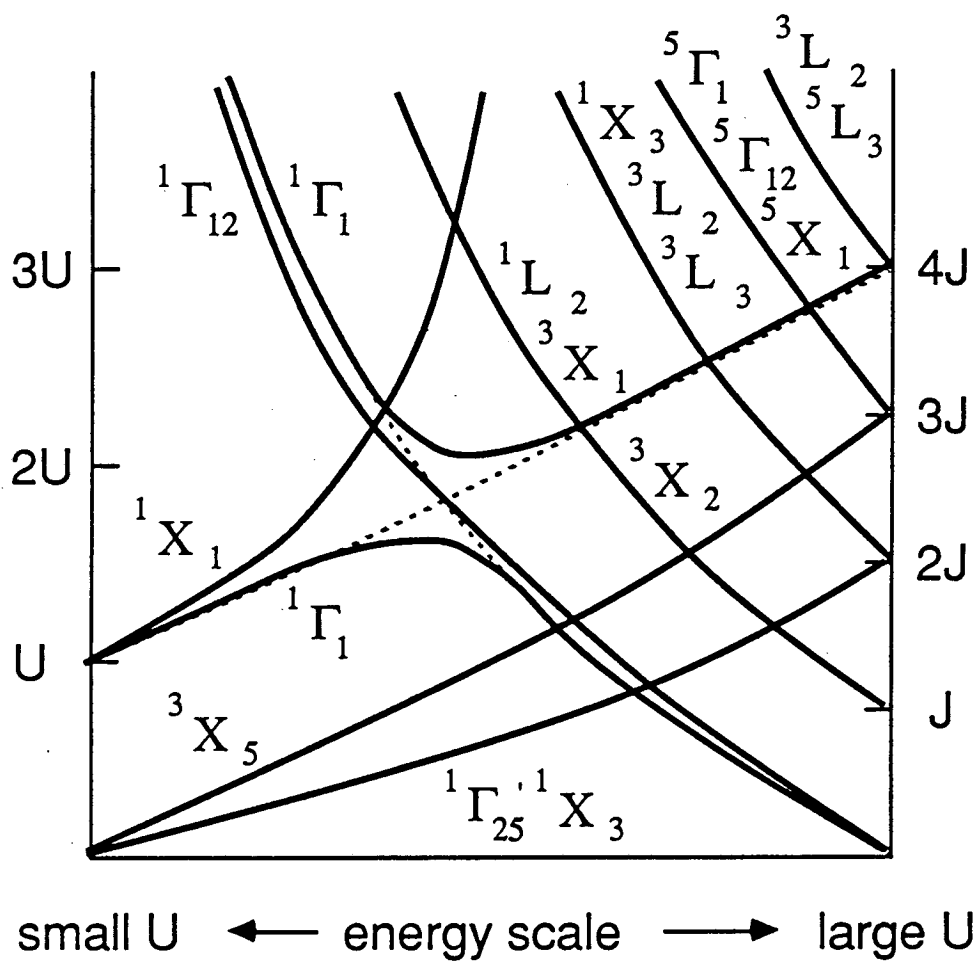
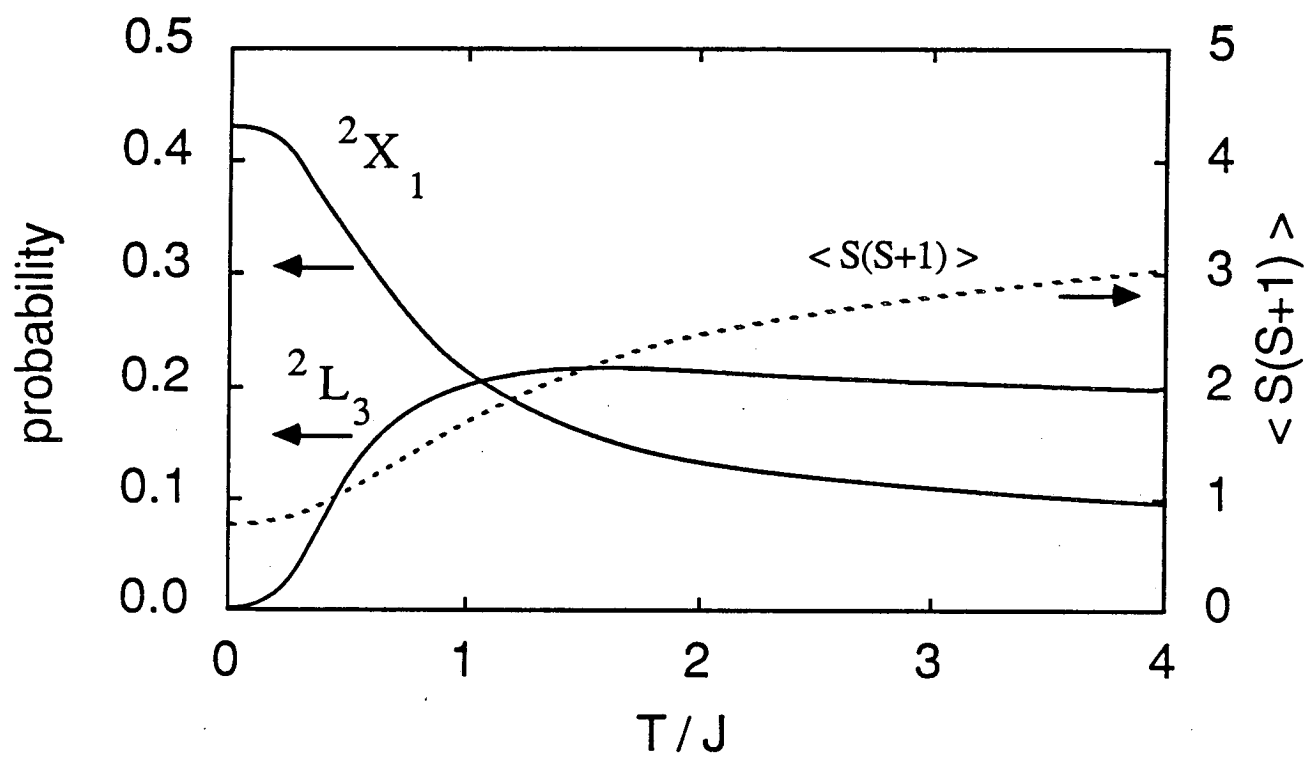


Figure 4.



LAWRENCE BERKELEY LABORATORY
TECHNICAL INFORMATION DEPARTMENT
UNIVERSITY OF CALIFORNIA
BERKELEY, CALIFORNIA 94720